ELSEVIER
Nuclear Instruments and Methods in Physics Research B 147 (1999) 361–366
NIM B
Beam Interactions with Materials & Atoms

Homogeneously size distributed Ge nanoclusters embedded in SiO_2 layers produced by ion beam synthesis

A. Markwitz [a,*], L. Rebohle [a], H. Hofmeister [b], W. Skorupa [a]

[a] *Forschungszentrum Rossendorf, Institut für Ionenstrahlphysik und Materialforschung, P.O. Box 51 01 19, 01314 Dresden, Germany*
[b] *Max Planck Institute of Microstructure Physics, Weinberg 2, 06120 Halle/Saale, Germany*

Abstract

500 nm SiO_2 layers were implanted with 450 keV ($F = 3\times10^{16}$ at./cm^2) and 230 keV ($F = 1.8\times10^{16}$ at./cm^2) Ge ions at room temperature to obtain an almost constant Ge concentration of about 2.5 at.% in the insulating layer. Subsequently, the specimens were annealed at temperatures between 500°C and 1200°C for 30 min in a dry N_2 ambient atmosphere. Cross-sectional TEM analysis reveal homogeneously distributed Ge nanoclusters arranged in a broad band within the SiO_2 layer. Their mean cluster size varies between 2.0 and 6.5 nm depending on the annealing conditions. Cluster-free regions are always observed close to the surface of the specimens independent of the annealing process, whereas a narrow Ge nanocluster band appears at the SiO_2/Si interface at high annealing temperatures, e.g. $\geqslant$ 1000°C. The atomic Ge redistribution due to the annealing treatment was investigated with a scanning TEM energy dispersive X-ray system and Rutherford back scattering (RBS). © 1999 Elsevier Science B.V. All rights reserved.

Keywords: SiO_2; Ge; Nanoclusters; TEM

1. Introduction

As a basic electronics material bulk single-crystalline Si is of limited use for optoelectronic applications due to its low intrinsic recombination probability. Recently it has been demonstrated that Si-based nanostructures can yield high-intensity photoluminescence (PL) at room temperature. After promising PL results from porous Si produced by wet etching [1], Si nanosystems have been produced by microwave plasma decomposition of SiH_4 and H_2 [2], rf-magnetron sputtering of Si and SiO_2 [3], laser breakdown of silane gas [4], and crystallisation of amorphous Si [5]. One of the most promising methods of producing nanometer-sized structures bases on ion implantation of Si [6–11] or Ge [12–15] into an SiO_2 matrix and subsequent heat treatment, because of a precise control over the quantities and depth distributions of the implanted ions, which allows full compatibility with the Si technology.

Whereas most of the former investigations reported about PL in the red spectral region

* Corresponding author. Present address: The Institute of Geological and Nuclear Sciences Limited, 30 Gracefield Road, P.O. Box 31312, Lower Hutt, New Zealand. Tel.: +64 4 570 4785; fax: +64 4 570 4657; e-mail: a.markwitz@gns.cri.nz

PII: S0168-583X(98)00542-4

[7,10,12,13], recent results demonstrate the possibility to extract blue PL from Si and Ge implanted SiO_2 [15–17]. There are also first reports on EL from Si [18–20] and Ge implanted [21–24] SiO_2. Last year EL measurements revealed strong luminescence in the blue spectral region with a quantum power efficiency of 5×10^{-4} [24], which is of general interest in finding a direct link between Si-based micro-and optoelectronics. However, up to now, the origin of this blue luminescence is still under debate. To get more information about this missing link between the luminescence and microstructure, the atomic distribution of Ge and its relation to Ge nanoclusters is investigated in this work as a function of implantation and annealing conditions. Furthermore, the possibility in forming homogeneously distributed Ge nanoclusters with nearly the same size in the SiO_2 layer by using double-energy implantation and standard furnace annealing in dry N_2 ambient is investigated too.

In most cases single-energy implantations are used, which result, however, always in a nearly Gaussian shaped depth distribution of the implanted ions and largely unequal conditions for the nucleation and growth of the second-phase inclusions. Therefore, nucleation occurs preferentially around the peak of the implantation profile. For example, the size of the nanoclusters varies between 2 and 10 nm if implanting 350 keV Ge^+ions into 500 nm SiO_2 layers with $F=5\times10^{16}$ at./cm^2 and annealing the specimen at 1100°C for 1 h in dry N_2 ambient, subsequently [25]. This disadvantage can be nearly completely avoided when using multiple-energy implantations, as they enable the production of a thicker impurity-rich layer of better uniformity to increase the number of clusters/emitting centres. Several investigations have shown an increase of the mean cluster size with increasing annealing temperature [25,26]. However, the existence of nanoclusters is sometimes concluded only from Ge depth distributions measured with RBS [21], which is ambiguous. Only detailed cross-sectional TEM studies can provide this information on nanostructuring at the atomic scale. Additionally, energy dispersive X-ray scanning TEM analysis (STEM-EDX) enables the measurement of the Ge depth profiles with a high depth resolution in each analysis depth, which is the major advantage of STEM-EDX analysis [26] compared to standard RBS measurements.

2. Experimental

500 nm thick SiO_2 layers were grown on flat-surface single-crystalline Si substrates in a wet ambient at 1000°C. Afterwards, the insulating layers were implanted with 450 keV Ge^+ions ($F=3\times10^{16}$ ions/cm^2) and 230 keV Ge^+ions ($F=1.8\times10^{16}$ ions/cm^2) at room temperature in order to achieve an almost constant Ge concentration in the SiO_2 layer, refrained from the near-surface region and a decreasing Ge amount at the SiO_2/Si interface. Post-implantation annealing was performed in the temperature range from 500°C to 1200°C for 30 min in a dry N_2 ambient in a standard furnace to initiate Ge nanoclustering. A PHILIPS CM300 transmission electron microscope with a line resolution of 0.14 nm was used for TEM analyses of cross-sectional specimens prepared conventionally [26]. Additionally, STEM-EDX was used to measure the depth profiles of Ge, Si, and O, simultaneously [27].

3. Results and discussion

Fig. 1 shows the alteration of the Ge depth distributions by applying a subsequent annealing at 800°C and 1200°C for 30 min, respectively, as measured with STEM-EDX. The spectrum of the as-implanted specimen is plotted, additionally. As can be seen in the figure by the shape of the Ge depth distribution of the as-implanted specimen, the Ge double-energy implantation with 230 and 450 keV leads to an almost homogeneous Ge amount in the SiO_2 layer, within a depth range of 100–350 nm. This is about half of the thickness of the entire SiO_2 layer, where RBS measurements yield an average Ge concentration of 2.5 ± 0.2 at.%. At the SiO_2/Si interface, the Ge concentration drops below 0.5 at.%, but Ge is detected up to a depth of about 600 nm, where the detection limit of standard RBS (1.7 MeV $^4He^+$) of about 0.1 at.% is achieved. For the Ge depth profiles measured with STEM-EDX, the depth scales are

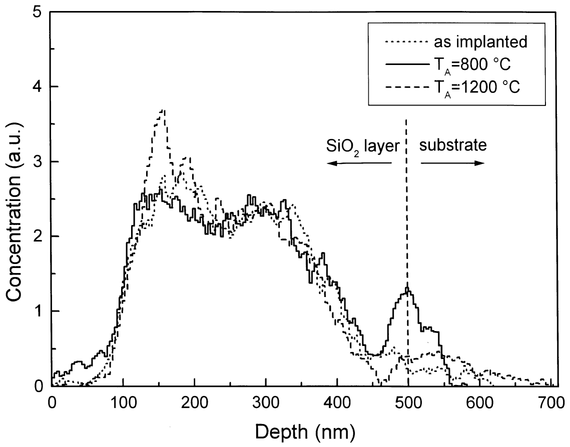

Fig. 1. Distribution of implanted Ge after annealing as a function of the annealing temperature measured with STEM-EDX. The Ge implantations into 500 nm SiO_2 layers were performed with 450 keV ($F = 3\times10^{16}$ at./cm^2) and 230 keV ($F = 1.8\times10^{16}$ at./cm^2) Ge^+ ions at room temperature.

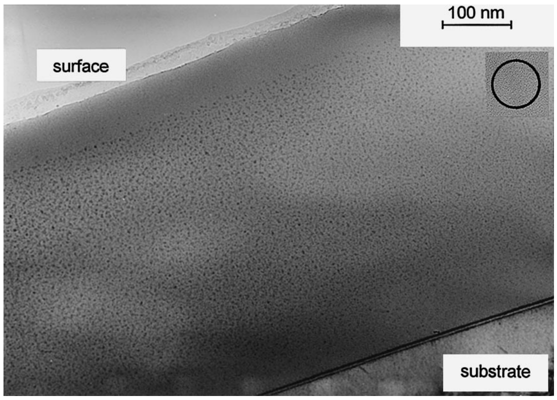

Fig. 2. TEM micrograph of the specimen annealed at 800°C for 30 min (implantation parameters ref. to Fig. 1). A crystalline Ge nanocluster is shown in the inset.

adjusted by the signals of O and Si of the SiO_2 layer and the Si substrate, whereas the concentration values are obtained from RBS measurements.

After annealing, the shape of the Ge depth distributions remained almost box-like up to the temperature of 800°C. However, at this temperature, a Ge peak appears at the SiO_2/Si interface in the STEM-EDX and RBS spectra and becomes more and more pronounced with increasing annealing temperature (up to 1100°C), but finally, disappears again at 1200°C. Theoretically, this Ge peak at the SiO_2/Si interface is a consequence of the Ge diffusion in the SiO_2 layer during annealing, where the SiO_2/Si interface acts as a very effective sink for dissolved Ge in SiO_2. An extensive theoretical description of Ge nanoclusters in SiO_2 produced by ion beam synthesis including supersaturation, nucleation, growth, and Ostwald ripening will be published in [28].

The dependence of nanoclusters within the SiO_2 layer and at the SiO_2/Si layer on the annealing process and their relation to the atomic Ge distributions are studied with cross-sectional TEM.

Fig. 2 shows a TEM micrograph of a specimen annealed at 800°C for 30 min (Ge depth profile ref. to Fig. 1) obtained with a reduced electron energy of 110 keV in order to enhance the Z contrast. Close to the surface of the specimen, a nanoclusters-free region is observed (thickness 115 nm) being in agreement with the low Ge amount of <1 at.% in the Ge depth distribution. However, Ge nanoclusters appear in the centre of the SiO_2 layer. Their typical size is 2 nm and they are arranged in a broad band, which covers about 80% of the entire SiO_2 layer. It has to be pointed out, that the size of the Ge nanoclusters in the broad band is almost the same. Strong deviations from the mean cluster size are not measured as in the case of a single-energy Ge implantation with 350 keV into 500 nm SiO_2 layers under comparable conditions [25,26]. As can be seen in the inset in Fig. 2 obtained with the electron energy of 300 keV, the Ge nanoclusters are crystalline and their (1 1 1) lattice planes can be identified. A lattice parameter of 0.31 nm is calculated from the observed lattice spacing. This value is about 5% lower than the one of Ge bulk material. Deviations of lattice parameters from bulk values are often measured for small particles, e.g., 5% smaller for Si nanoclusters embedded in SiO_2 layers produced by magnetron sputtering [29]. Following the broad nanocluster band, another cluster-free region with a thickness of about 40 nm is observed in the TEM micrographs in direction to the SiO_2/Si interface. It has to be noticed, that Ge nanoclusters are already found at lower annealing temperatures of 500°C and 700°C, but not in as-implanted specimens. However, these nanoclusters are not crystalline, as investigated with high resolution TEM (HRTEM) and dark field imaging.

In addition to the observation of the broad nanocluster band in the SiO_2 layer, a damage band in the Si substrate is observed in the TEM micrographs. It is caused by the high-energy implantation using an ion energy of 450 keV. The range of the damage in the Si substrate is 70 nm, which corresponds well with TRIM calculations revealing a critical nuclear energy deposition of $S_n^{crit} = 10^{24}$ eV/cm^{-3} in this depth, that is necessary for disordering the crystalline structure of the Si substrate. The damaged region recrystallises during annealing as a function of the annealing time when applying temperatures $\geqslant 700$°C. For example, after annealing at 800°C for 30 min, the former amorphous region has crystallised, however, a band of dislocations remains at the position of the end of range defects.

In Fig. 3, a TEM micrograph of the specimen annealed at 1200°C is shown. Ge nanoclusters are already visible in the overview micrograph and in the insets ((a) micrograph obtained in dark field mode, (b) high resolution micrograph of Ge nanocluster). Their size varies between 4.5 and 8 nm (mean cluster size 6.5 nm) and they are arranged in a broad band within the SiO_2 layer, covering about 80% of the insulating layer, which is in agreement with the nanoclusters presented in Fig. 2. The crystallinity of the nanoclusters is shown in inset (a) by bright spots in the dark field micrograph indicating reflexes of the (1 1 1) lattice planes. As in the case of the specimen annealed at 800°C, the cluster-free region in the upper part of the SiO_2 layer corresponds to the absence of Ge in the depth distribution, as measured with STEM-EDX. However, in contrast to the specimen annealed at 800°C a narrow Ge nanocluster band appears in the SiO_2 layer very close to the SiO_2/Si interface.

Fig. 4 shows a more detailed micrograph of the narrow nanocluster band at the SiO_2/Si interface with a thickness of about 10 nm. This band is located in the SiO_2 layer and in a distance of about 10 nm from the SiO_2/Si interface. The crystallinity

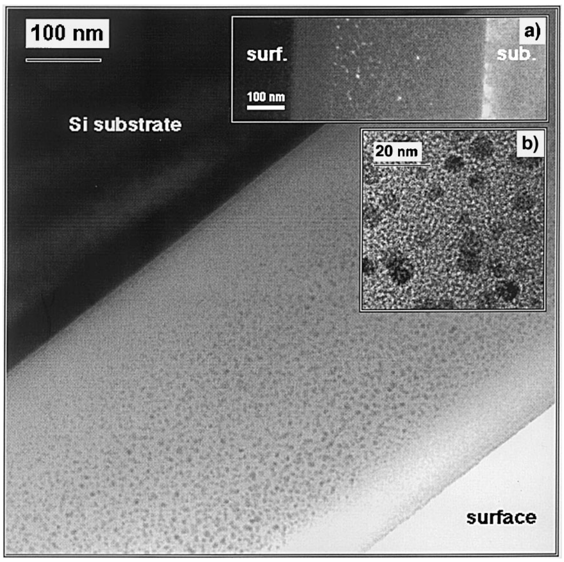

Fig. 3. TEM micrograph of the specimen annealed at 1200°C for 30 min (implantation parameters ref. to Fig. 1). Inset (a) shows a dark field micrograph of the specimen indicating the crystallinity of the nanoclusters, whereas the almost homogeneously size of the nanoclusters is shown in inset (b).

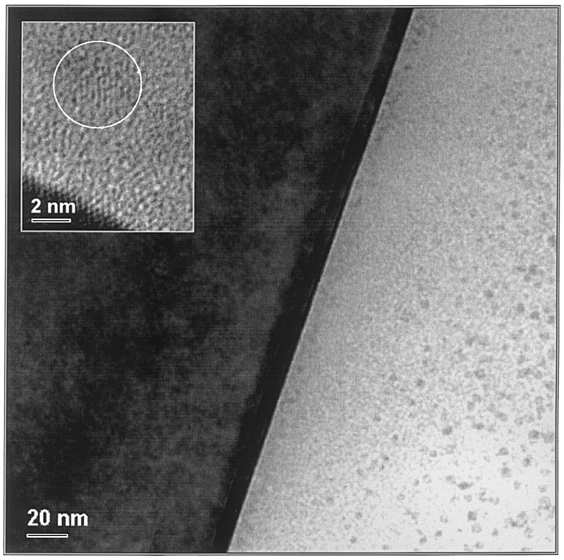

Fig. 4. Detailed TEM micrograph of the nanocluster band located close to the SiO_2/Si interface. The crystallinity of the nanoclusters is shown in the inset.

of the Ge nanoclusters can be seen in the inset in Fig. 4 by the observation of (1 1 1) lattice planes with the spacing of 0.31 nm, which is the same for all the nanoclusters. It has to be noted, that such Ge nanocluster bands are also observed in specimens annealed at 1000°C and 1100°C. First theoretical calculations [28] indicate that the formation of this very narrow Ge nanocluster band is strongly related to the Ge diffusion in SiO_2 layer during annealing and the acting of the SiO_2/Si interface as a very effective sink for dissolved Ge atoms in SiO_2.

Finally, it has to be noted, that these implanted and subsequently annealed SiO_2 layers exhibit strong PL in the blue spectral region [30]. Although, the intensity of the PL is correlated with the mean Ge nanocluster size and decreases with increasing nanocluster size, which is found by comparing PL and cross-sectional TEM investigations, its origin is still under debate. However, combined analysis indicate that the outer shell of the Ge nanoclusters, where Ge is bonded to GeO_x, plays a significant role for the strong blue PL.

4. Summary

Cross-sectional TEM investigations show the possibility of forming Ge nanoclusters with almost the same size by double-energy implantation into 500 nm SiO_2 layers and subsequent annealing at appropriate high temperatures. These Ge nanoclusters are single crystalline when applying annealing temperatures $\geqslant 800°C$. Their typical sizes vary between 2.0 and 6.5 nm and they are arranged in a broad band within the SiO_2 layer, covering about 80% of the insulating layer. The appearance of the Ge nanoclusters is correlated with the Ge amount in the SiO_2 layers, as investigated with STEM-EDX and RBS Cluster-free regions are always observed close to the surface of the specimens as a result of the low Ge concentration in this part of the SiO_2 layer. A narrow Ge nanocluster band with a thickness of about 10 nm appears additionally close to the SiO_2/Si interface in the SiO_2 layer at the distance of about 10 nm at high annealing temperatures, e.g. $\geqslant 1000°C$.

References

[1] L.T. Canham, Appl. Phys. Lett. 57 (1990) 1046.
[2] H. Takagi, H. Owada, Y. Yamazaki, A. Ishizaki, T. Nakagiri, Appl. Phys. Lett. 56 (1990) 2379.
[3] K. Kohno, Y. Osaka, F. Toyomura, H. Katayama, Jpn. J. Appl. Phys. 33 (1994) 6616.
[4] Y. Kanemitsu, T. Ogawa, K. Shiraishi, K. Takega, Phys. Rev. B 48 (1993) 4883.
[5] T. Shimizu-Iwayama, K. Fujita, S. Nakato, K. Saitoh, T. Fujita, N. Itoh, J. Appl. Phys. 75 (1994) 7779.
[6] X. Zhao, O. Schoenfeld, J. Kusano, Y. Ayogai, T. Sugano, Jpn. J. Appl. Phys. 33 (1994) 649.
[7] H.A. Atwater, K.V. Shcheglov, S.S. Wong, K.J. Valahala, R.C. Flagan, M.L. Brongersma, A. Polman, Mater. Res. Soc. Symp. Proc. 321 (1994) 363.
[8] J.G. Zhu, C.W. White, J.D. Budai, S.P. Withrow, Y. Chen, Mat. Res. Soc. Symp. Proc. 358 (1995) 175.
[9] T. Komoda, J.P. Kelly, A. Nejim, K.P. Homewood, P.L.F. Hemment, B.J. Sealy, Mater. Res. Soc. Symp. Proc. 358 (1995) 163.
[10] P. Mutti, G. Ghislotti, S. Bertoni, L. Bonoldi, G.F. Cerofolini, L. Meda, E. Grilli, M. Guzzi, Appl. Phys. Lett. 66 (1995) 851.
[11] W. Skorupa, R.A. Yankow, I.E. Tyschenko, H. Fröb, T. Böhme, K. Leo, Appl. Phys. Lett. 68 (1996) 2412.
[12] C.M. Yang, K.V. Shcheglov, M.L. Brongersma, A. Polman, H.A. Atwater, Mater. Res. Soc. Symp. Proc. 358 (1995) 181.
[13] K.V. Shcheglov, C.M. Yang, K.J. Vahala, H.A. Atwater, Appl. Phys. Lett. 66 (1995) 745.
[14] H.A. Atwater, K.V. Shcheglov, S.S. Wong, K.J. Vahala, R.C. Flagan, Mater. Res. Soc. Symp. Proc. 316 (1994) 409.
[15] L. Rebohle, I.E. Tyschenko, H. Fröb, K. Leo, R.A. Yankow, J.v. Borany, G.A. Kachurin, W. Skorupa, Microelectron. Eng. 36 (1997) 107.
[16] L.S. Liao, X.M. Bao, X.Q. Zheng, N.S. Li, N.B. Min, Appl. Phys. Lett. 68 (1996) 850.
[17] X.M. Bao, T. Gao, F. Yan, S. Tong, Mater. Res. Soc. Symp. Proc. 438 (1997) 477.
[18] L.S. Liao, X.M. Bao, N.S. Li, X.Q. Zheng, N.B. Min, Solid State Commun. 97 (1996) 1039.
[19] H.Z. Song, X.M. Bao, N.S. Li, J.Y. Zhang, J. Appl. Phys. 82 (1997) 4028.
[20] F. Kozlowski, H.E. Porteanu, V. Petrova-Koch, F. Koch, Mater. Res. Soc. Proc. 452 (1997) 657.
[21] J.Y. Zhang, X.L. Wu, X.M. Bao, Appl. Phys. Lett. 71 (1997) 2505.
[22] L. Rebohle, I.E. Tyschenko, J.v. Borany, B. Schmidt, R. Grötzschel, A. Markwitz, H. Fröb, R.A. Yankov, W. Skorupa, Mat. Res. Soc. Symp. Proc. Fall Meeting 1997, Dec. 1–5, 1997, Boston, USA.
[23] L. Rebohle, J.v. Borany, R.A. Yankow, W. Skorupa, I.E. Tyschenko, H. Fröb, K. Leo, Appl. Phys. Lett. 71 (1997) 2809.

[24] L. Rebohle, J.v. Borany, R. Grötzschel, A. Markwitz, B. Schmidt, I.E. Tyschenko, H. Fröb, K. Leo, Phys. Stat. Sol. (a) 165 (1998) 31.
[25] A. Markwitz, B. Schmidt, W. Matz, R. Grötzschel, A. Mücklich, Nucl. Instr. and Meth. B 142 (1998) 338.
[26] J.v. Borany, R. Grötzschel, K.H. Heinig, W. Matz, A. Markwitz, B. Schmidt, W. Skorupa, Appl. Phys. Lett. 71 (1997) 3215.
[27] A. Markwitz, W. Matz, B. Schmidt, R. Grötzschel, Surf. Interf. Anal. 26 (1998) 359.
[28] K.H. Heinig, B. Schmidt, A. Markwitz, R. Grötzschel, M. Strobel, Nucl. Instr. and Meth. B, to be published.
[29] H. Seifarth, R. Grötzschel, A. Markwitz, W. Matz, P. Nitzsche, L. Rebohle, Thin Solid Films 330 (1998) 202.
[30] L. Rebohle, J.v. Borany, A. Markwitz, W. Skorupa, paper presented at this conference.